

# Hierarchical Markovian modeling of multi-time systems

M. Abel<sup>1</sup>, K.H. Andersen<sup>2</sup> and G. Lacorata<sup>3</sup>

<sup>1</sup> Universität Potsdam, Institut für Physik,  
Postfach 601553, D-14415 Potsdam, Germany.

<sup>2</sup> Dept. of Mechanical Engineering, Technical University of Denmark,  
DK-2800 Kgs. Lyngby.

<sup>3</sup> Dipartimento di Fisica, Università dell'Aquila,  
Via Vetoio 1, I-67010 Coppito, L'Aquila, Italy.

January 6, 2022

## Abstract

We present a systematic way to analyze and model systems having many characteristic time-scales. The method we propose is employed for a test-case of a meandering jet model manifesting chaotic tracer dispersion with long time-correlations. We first choose a suitable state space partition and analyze the symbolic dynamics associated to the fluid particle position. In a second step we construct a stochastic process in terms of a multi-time Markovian model. This corresponds to a hierarchy of random travelers on a graph where each traveler moves at his own time scale. The results are compared on the basis of statistical measures such as entropies and correlation functions.

## 1 Introduction

Extended systems, as they are found in nature, often show complicated dynamics on several characteristic scales and times. One, often cited, example is turbulent motion, where the dynamics stretches from an integral scale to the dissipation scale. In many situations, it is possible to find a low-order approximation of the dynamics and one remains with the task to describe the temporal behavior of the system under consideration. A standard example is the area of pattern formation [1] where one ends up with systems of ordinary differential equations, describing the evolution of a few spatial modes. It is, however, not always possible to perform a mode decomposition, but nevertheless spatial

structure is clearly present. Then it makes sense to identify states and investigate the dynamics and interaction of these states. There exists a huge amount of works concerning deterministic [2], and stochastic modeling [3]. Examples for the above mentioned systems are found among others in climatology [4], oceanography [5], or ecosystems [6]. In these examples, one typically follows tracer particles that are put into the respective flow and performs some partitioning afterwards. We do not want to bother with this first, very subtle step of partitioning, rather we take the partition as given.

On the other hand, there exist systems where one directly observes the temporal signal of several states, which can be coupled. A partitioning is then obviously not necessary and one is not bothered anymore with the problems arising from that point. Examples are systems of coupled oscillators, coupled ODE's. Between the two described scenarios lie numerical simulations where it is often easy to identify spatial states by physical [7, 8] or mathematical [9] arguments.

Often, one considers coupled systems with one dominant time scale and different typical amplitudes. States with fast oscillations are usually assumed to have small amplitude and are neglected. This way, small oscillations that might well play a role in inducing finite-size perturbations and chaos in a system are neglected. On the other hand, it can well appear that the fast fluctuations have large amplitude and thus obscure the slow states dynamics.

Chaoticity of nonlinear systems implies the loss of memory of a tracer that moves in the (either extended or discrete) system. It thus makes sense to use a statistical description. In this article, we present a way to treat systems with several states, which are possibly coupled and act on different time scales. We explain a method to filter time signals and extract information at different time scales along with a non-conventional, general method to construct a stochastic model capable to approximate the evolution of the system under observation. We end up with a statistical description of a multi time scale dynamics in terms of a Markovian cascade process. The different time scales are identified and the dynamics is reconstructed in the statistical sense. This is done in order to compare the reconstructed and original dynamics by means of complexity measures and correlation functions to ensure that the modeling is sensible. Apart from the theoretical interest about how to formulate a statistical model, we can figure out mainly two practical uses: firstly, one can implement a statistical model as a building block in geophysical or other large scale simulations to get an idea of the fast (and possibly small) scale fluctuations and secondly, one could use transition times and probabilities between different states to evaluate the most probable traces a passive scalar (e.g., a contaminant) would have in the described flow (e.g., the atmosphere).

In this article we treat an example from geophysics: the chaotic dispersion process generated from a meandering jet model. Apart from the interest in itself, we believe that this system is worth noting for the following reasons: *i)* it shows chaos and mixing on two time scales as desired by our research goal (and thus represents some minimal setting giving the possibility for detailed studies of the methods we developed), *ii)* it is typical for geophysical applications *iii)*

we can compare results explicitly, since there exists an older article attempting to solve the task with conventional methods.

The article is organized as follows: After this brief introduction, we present in Section 2 the model, in Section 3 the analysis method is explained, in Section 4 the construction of the model trajectory is described, Section 5 contains the results and the comparison of constructed and original signal, finally we end with a short discussion and some conclusions in Section 6.

## 2 The model: a signal with different characteristic times

Let us consider a simple but non-trivial case of multi-time dynamics in a geophysical system: Lagrangian transport across a meandering jet, formerly introduced as kinematic model of the Gulf stream by Bower [10] and Samelson [11]. The model serves our purposes, since it can be well used as the test case in which only two characteristic times are involved as we will see below (i.e. fast and slow particle transitions across the flow). In this model, the gulf stream is represented by a central meandering jet, flanked by gyres rotating in opposite directions (Fig. 1). The model is described by the stream function [10, 11]:

$$\Psi(x, y) = -\tanh \frac{y - B_0 \cos(kx)}{\sqrt{1 + B_0^2 k^2 \sin^2(kx)}} + cy, \quad (1)$$

where  $x$  and  $y$  are the spatial coordinates of a fluid particle,  $k$  is the spatial wave number of the meander structure,  $B_0$  controls the amplitude of the meanders, the term in the denominator of (1) defines the width of the jet and  $c$  is the velocity in the “far field” north and south of the (westerly) jet current. The fluid particle velocity components  $(u, v)$  at the point  $(x, y)$  are:

$$u = -\frac{\partial \Psi}{\partial y}, \quad \text{and} \quad v = \frac{\partial \Psi}{\partial x}. \quad (2)$$

Chaos is introduced by adding an explicit time dependence to the stream function (1) by replacing  $B_0$  with  $B(t)$  defined as

$$B(t) = B_0 + \epsilon \cdot \cos(\omega t + \theta) \quad (3)$$

This induces a periodic oscillation of the meander, with period  $T = 2\pi/\omega$ , amplitude  $\epsilon$  and initial phase  $\theta$ , around the mean value  $B_0$ . Depending on the values of the perturbation parameters,  $\omega$  and  $\epsilon$ , chaotic motion occurs in the vicinity of the separatrices. For appropriate values of the perturbation parameters, resonance overlap [12] occurs, and transport between northern and southern gyre can take place.

A study of Lagrangian trajectories in one elementary cell of the streamline pattern shows that there are two basic time scales:  $\tau_g$  which is the advection time of a particle traveling along the jet core, and  $\tau_o = 2\pi/\omega$  which is the

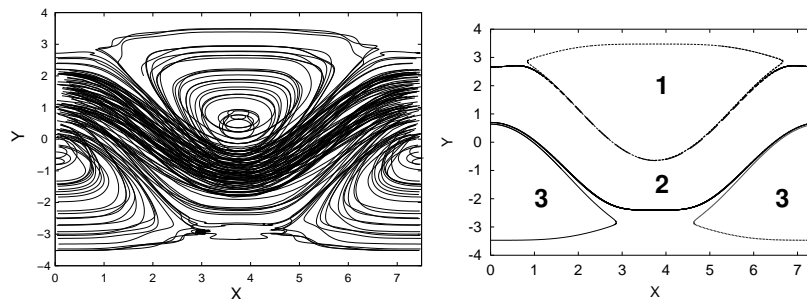


Figure 1: Left: snapshot of the streamlines in the meandering jet model (1). The gyres are seen as closed orbits to the north and south of the jet. The boundary between the jet and the gyres, as defined here, correspond to  $\Psi = \pm 0.60$ . Spatial coordinates are measured in units of the wavelength  $2\pi/k$ . Right: a particle trajectory (periodic boundary conditions). In the corresponding gulf stream system the particle experiences an average drift from the left to the right. The tracer can be caught by a gyre (states 1 and 3) or the jet (state 2) for a longer time (dense tracks).

period of the oscillation of the meander. In the following, in order to obtain non-dimensional equations we rescale time with  $\tau_o$ . The particle position is sampled accordingly at the end of each period.

A coarse graining of the space can be obtained by dividing the flow domain into *elements*, e.g., separating regions with closed from regions with open streamlines. The partition to be used throughout this article is defined as: 1) the northern gyre, 2) the jet, 3) the southern gyre (cf. Fig. 1). Assigning each of the partition a number yields a discrete description of the trajectory.

An example of a particle trajectory is seen in Fig. 1. For this example (and the rest of this article) the parameters of the models have been chosen as: meander wavelength  $l_0 = 2\pi/k = 7.5$ , the (mean) meander amplitude  $B_0 = 1.2$  and  $c = 0.12$ . An example of the corresponding trajectory in terms of the partitions is seen in Figure 4, top line. The trajectory consists of fast oscillations between one of the gyres and the jet, interleaved by periods where it stays in one of the gyres for a longer time. The fast oscillations are basically due to the fact that the particle undergoes a large number of crossings back and forth across the boundary of two partitions.

### 3 Entropic analysis and filtering

The aim of this section is the presentation of a suitable filtering technique which allows to highlight and characterize the dynamical features at different characteristic times. This filtering method, developed on the basis of an exit time approach to entropy computation, is a way to understand how to find a good

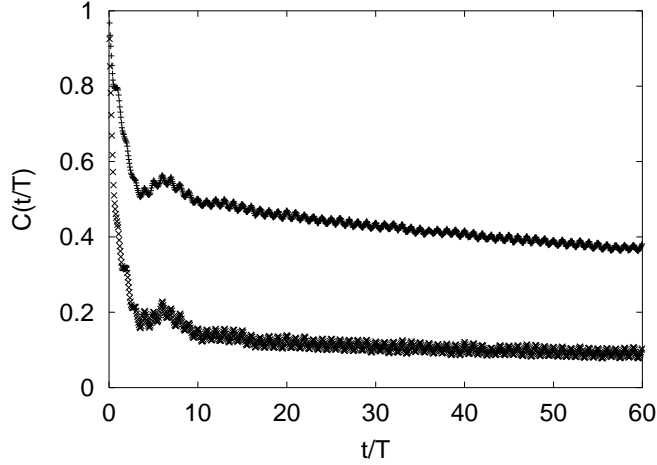


Figure 2: Correlation function of the signal shown in Fig. 4, top graph. The long-time correlations are clearly present but cannot be captured by a usual Markov chain with equidistant time steps.

stochastic model for the process.

### 3.1 Encoding of the signal

Let us consider the time signal of an observable  $s(t)$ . Typically  $s(t)$  is registered at a certain sampling rate  $\tau_s^{-1}$ , i.e., we consider a discrete time evolution,  $s(n)$  with  $t = n \cdot \tau_s$ . A coarse-grained description of  $s(n)$  is obtained by dividing the range of  $s(n)$  through a partition with, say,  $P$  elements, and assigning a label to each element of the partition, say  $\sigma_1, \sigma_2, \dots, \sigma_P$ . Consequently, the time evolution of  $s(n)$  is mapped into a symbolic dynamics  $\sigma(n)$ , with  $\sigma(n) \in \{\sigma_1, \sigma_2, \dots, \sigma_P\}$ . Let us indicate with  $\sigma$  a generic symbol of the sequence and with  $\tau$  the lifetime of  $\sigma$ , i.e., the time the system takes to move from the state  $\sigma$  into a new one. We will use sometimes the terms residence time or exit time as a synonym for “lifetime” when more suitable, in the context of markov chains, the term waiting time is used (mainly in the literature of queuing systems).

A sequence of length  $n$  is designated as follows:

$$S_n = (x_1, x_2, \dots, x_n), \quad \text{where} \quad (4)$$

$$x_i = (\sigma_i, \tau_i). \quad (5)$$

For example, imagine a signal  $s(t) = (1, 1, 1, 2, 2, 2, 2, 3, 3, 1, 1, \dots)$  which assumes positive integer values at each unit time step ( $\tau_s = 1$ ); then the corresponding  $(\sigma, \tau)$  variables are  $\sigma_i = (1, 2, 3, 1, \dots)$  and  $\tau_i = (3, 4, 2, 2, \dots)$ , respectively.

### 3.2 Estimating Entropies

Let us briefly remind some recent results concerning the development of the estimation of entropy using the exit-time approach [13, 14]. To illustrate the basic ideas we describe the method and afterwards discuss its application to the problem under consideration, some details are explained in the appendix.

Out of the set of sequences  $S_n$  we collect statistics for each subsequence  $S_n$  and construct the probability distribution  $P(S_n)$ . Now, one can compute the Shannon entropy  $h$  of the signal  $\sigma$  by the following identity:

$$h = \frac{h^*}{\langle \tau \rangle} \quad (6)$$

where  $h^*$  is the Shannon entropy of  $x_n$ ,  $h^* = \lim_{n \rightarrow \infty} H_{n+1}^* - H_n^*$  (the information production with  $n$ ), with

$$H_n^* = - \sum_{S_n} P(S_n) \ln P(S_n), \quad (7)$$

and  $\langle \tau \rangle$ , the average life time, is computed as

$$\langle \tau \rangle = \lim_{N \rightarrow \infty} \frac{1}{N} \sum_{i=1}^N \tau_i \quad (8)$$

Denoting the entropies of the  $\sigma$  and  $\tau$  sequences with  $h^*(\sigma)$  and  $h^*(\tau)$ , respectively, one can determine upper and lower bounds on the entropy:

$$\max[h(\sigma), h(\tau)] < h(\sigma, \tau) < h(\sigma) + h(\tau) \quad (9)$$

The details of the method are described in [13, 14].

### 3.3 The filtering procedure

Let us now introduce a procedure to select the temporal behavior “slower than a given frequency”. The filter should therefore be able to discard the many fast fluctuations from one state to another which occur very frequently (see figure 4, top line). We call this filter “killing window”; it operates in the following way. If the signal fluctuates from one state into another state before returning to the first state, and if this fluctuation lasts for a shorter time than  $\tau_F$  (the filter length of the killing window), this fluctuation is ignored. Written symbolically this means that:

$$(\sigma_1, \tau_1), (\sigma_2, \tau_2), (\sigma_1, \tau_3) \rightarrow (\sigma_1, \tau_1 + \tau_2 + \tau_3), \quad (10)$$

provided that  $\tau_2 < \tau_F$ . The effect of the algorithm is shown in Fig. 3, and the role of different lengths of killing windows is shown in Fig. 4. This filter has the effect of “killing” all fluctuations smaller than  $\tau_F$ . Note that it is also effectively prolongs the slower oscillations, c.f. Fig. 3.

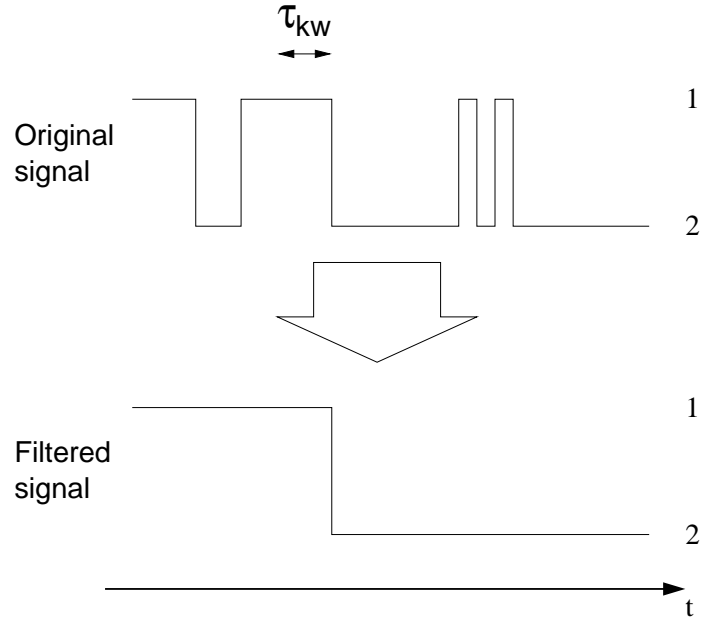


Figure 3: An illustration of how the killing window algorithm changes the original signal (top) to a filtered signal (bottom). In this example the signal is only alternating between two states, 1 and 2.

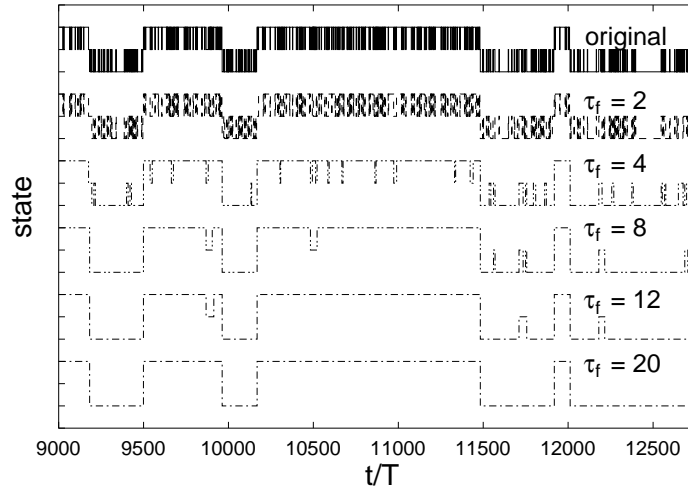


Figure 4: Comparison of signals filtered with different killing windows,  $\tau_F = 0, 2, 4, 8, 12, 20$ , from top to bottom. It is evident how the fast fluctuations are removed by the killing window. For a very long killing window,  $\tau_F = 20$ , also the residence in the jet is killed, and the model has effectively only two states.

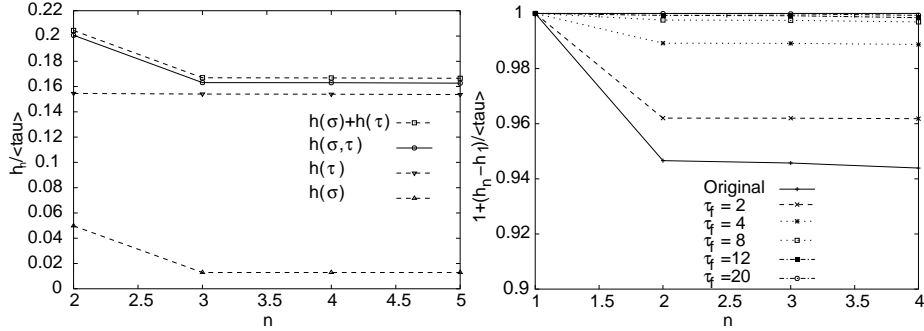


Figure 5: Calculation of the entropies. a) the entropy for  $\tau_F = 2$  together with the upper and lower bounds from (9). b) Comparison of the entropy for varying widths of the killing window. The entropies are normalized by adding a constant such that  $h_1 = 1$ .

With this filtering procedure applied to the original signal  $x_n$ , we obtain a filtered sequence  $x_n^{\tau_F}$ , for which we can compute the entropy  $h(\tau_F)$  using (6). We used for simplicity a filter that acts backwards in time. It is however not difficult to redefine the filter such as to be invariant under time reversal, the result remains the same within an error of the fast time scale. The observed signal varies over two very distant characteristic time scales,  $\tau_{fast}$  and  $\tau_{slow}$ , respectively. Thus, information at the slower time scale can be extracted if  $\tau_{slow} \gg \tau_F \gtrsim \tau_{fast}$ , because due to the second inequality almost all fast oscillations are killed.

In Fig. 5a the convergence of the entropy, at varying the block size, for a killing window of length 2 is shown, together with the upper and lower bounds from (9). First of all we see that the entropy lies nicely in between the upper and the lower bounds. For a killing window of length 2 this is not surprising, as most of the transitions are fast oscillations between jet and gyre. However, this entropy converges after  $n = 2$ , which means that one needs a second order Markovian process in order to properly describe this process. Let us stress that now the state of the system is given by  $\sigma$  and  $\tau$ , therefore a Markov model of order  $m$  corresponds, in the original space of the symbols  $\sigma$ , to a Markov model of order  $m \cdot \langle\tau/\tau_s\rangle$ . The entropy based only on the residence times,  $h(\tau)$ , is larger, and thus constitutes the effective lower bound for the total entropy. In Fig. 5b this is shown for the bare signal, and for killing windows of a length from 2 to 20. This entropy based on the residence times has converged immediately, which means that the residence times are basically uncorrelated. This is a sign for an exponential distribution to be confirmed below. Now, we have to decide the filter length for which the signal is described by a process on one time scale only. The killing window clearly destroys information. If the loss of information is proportional to the filter length, obviously the process is homogeneous (with respect to information loss) within the time scale we are considering. This



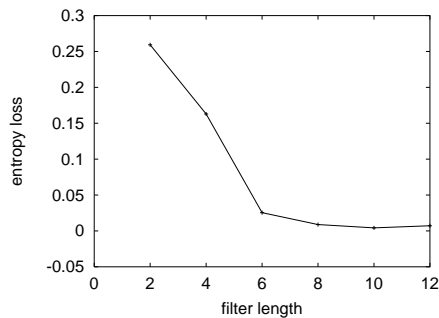


Figure 6: Information loss with filter length. From  $\tau_F = 8$  we have a constant rate of information loss and thus the difference between the different filter lengths is zero. This in turn justifies the description of the process by one scale only.

is analogous to the information production rate which has to converge to a constant to find the entropy of a chaotic system. [15]. In Fig. 6 we display the entropy loss depending on the filter length. For  $\tau_f = 8$  we have certainly reached convergence and thus the process can be described at the level of one single scale (namely the slow one). For completeness, we remark that almost all information is destroyed if the filter length exceeds the typical slow time scale,  $\tau_F \gtrsim \tau_{slow}$ .

## 4 Construction of the multiple time Markovian Model

In this section we will demonstrate how the analysis of the signal can be applied to construct a Markovian model, which can generate stochastic symbolic sequences with the same statistics as the original signal. The model should be able to reproduce both the slow and fast transitions. This is accomplished by first reproducing the slow scale signal, and then nesting the fast transitions into that one. We thus define a “horizontal” and a “vertical” dependence, the first describes the process on a specific time scale (slow or fast), the latter models the interdependencies between the different time scales. Both are assumed to be Markovian of first order, as our preceding analysis has shown, a generalization is straightforward. In the following, for the sake of clarity, we will use capital letters for slow scale and small ones for the fast scale.

### 4.1 Slow transitions

As determined by the Entropic analysis, the slow signal is the one filtered by a killing window of length  $\geq 8$ . The construction rules are the following:

- i) Given an entering state  $\sigma_I$  the process selects according to the transition probability matrix  $W_{IJ}$  its next state  $\sigma_J$ .
- ii) Given that selection of the transition  $IJ$ , the time spent in  $I$  before jumping to  $J$  is given by the random variable  $\tau_I$ , which in turn possesses the distribution  $P(\tau_I)$ .

Both needed informations are obtained from the filtered signal. By the given rules, we recognize that the construction concentrates on the *transitions* between states, rather than on the state itself. The *lifetime* of the states depends only on this transition, we see that the transition matrix does not include self-loops, like  $I \rightarrow I$  and thus has zeroes on the diagonal. In the case of independent lifetimes, i.e., exponential distribution, one can interchange steps i) and ii) and first select a state. Numerical examples for the matrices and residence times are given Section 5.

The reconstruction corresponds to a random traveler on a graph, which stays in each node with a certain node-characteristic time and then jumps over an edge to the next node according to a prescribed hopping probability.

## 4.2 Nesting of the fast scale

Up to now, the construction is rather standard. A new thing we introduce is the vertical connection between scales. The dynamics of the fast scale shall depend on the slow one, but apart from that be a first order Markovian process as described above by the rules i) and ii). The two quantities we have to consider are the pdf of the lifetimes  $p(\tau_i)$  and the transition probabilities  $w_{ij}$ . Both can be quite different from the slow processes quantities.

One obvious condition on the lifetimes is, that the duration of the fast states time intervals should not exceed the slow ones. This is fulfilled, since we anticipated a clear separation of time scales. In general, the transitions will be hit with an uncertainty of  $\langle \tau_{fast} \rangle \simeq \tau_F$ . This in accordance with the filtering analysis, which is only accurate up to the filter length. The lifetime distribution function  $p$  can be taken without any restrictions from the analysis, since we anticipate the times to be independent from each other (as confirmed for our example, see next section). The transition probabilities  $w_{ij}$ , however, have to be conditioned on the slow scale transitions and thus we have to write them for a complete description as  $w_{ij}(IJ)$ . Results are given in the next section.

We want to remark, again, that a first order in the space  $\sigma, \tau$  corresponds to a very high order in the space  $\sigma$  with conventional time sampling. For our illustration by the traveler on a graph we imagine the traveler moving with his own, slow speed, being accompanied by his dog which moves forth and back between the present node of the traveler and some other nodes he's allowed to visit. The dog rests only for short times in the nodes, and thus effectively moves at a fast time scale.

In conclusion, we have to find for each of the transitions  $IJ$  the according fast transition probability  $w_{ij}(IJ)$ . The fast process evolves then with the rules from  $w_{ij}(IJ)$  and the lifetime statistics  $p(\tau)$  within the window between two transitions.

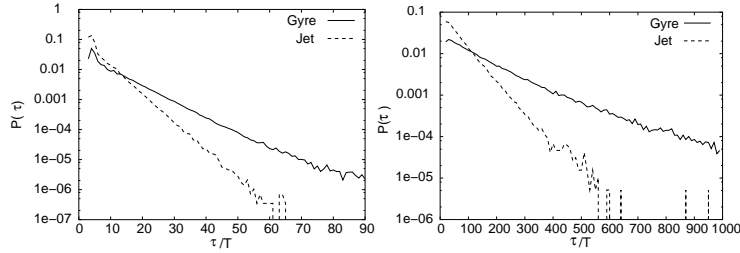


Figure 7: The pdf of the residence times in the jet and the gyres, calculated with a killing window of length 2 (left) and 12 (right).

In a generalized model,  $N$  different time scales are involved, then we order the processes from slowest to fastest time and construct the hierarchy by nesting the scale  $n$  into scale  $n - 1$ . This generalization is straightforward and will be reported elsewhere. Another generalization concerns Markov processes of higher order. This requires accurate bookkeeping of the dependencies but in principle is straightforward, too.

## 5 Results

In this section we will present how the technique described above compares to the real signal. The slow scale transition matrix, we obtain for our model

$$W_{IJ} = \begin{pmatrix} 0 & 0.65 & 0.35 \\ 0.5 & 0 & 0.5 \\ 0.35 & 0.65 & 0 \end{pmatrix}. \quad (11)$$

Note that due the symmetries of the meandering jet problem, this matrix could in principle be reduced to only its upper half. In general, this is however not the case. Since we have a very simple system with strong restrictions the fast transition matrices look simple, e.g., for  $w_{ij}(12)$ :

$$w_{ij}(12) = \begin{pmatrix} 0 & 1 & 0 \\ 1 & 0 & 0 \\ 0 & 0 & 0 \end{pmatrix}. \quad (12)$$

The residence times for the slow and fast scale are displayed in Fig. 7. Clearly they are very close to be exponential. This is a sign of a non-correlated process, which has also been found by the entropic analysis. From a fit to an exponential distribution we determine the mean residence time for the slow time scale to be  $\langle \tau \rangle_{slow,gyre} = 64.5$  and  $\langle \tau \rangle_{slow,jet} = 90.9$ , for the fast time scale we obtain  $\langle \tau \rangle_{fast,gyre} = 5.21$  and  $\langle \tau \rangle_{fast,jet} = 5.83$ , respectively.

For our example of a coarse grained spatial system, the trajectory, basically slowly drifts forth and back between north and south gyre, crossing the jet.

During this evolution, fluctuations occur about the boundaries of the states. Take, e.g., a trajectory starting at the northern gyre. Having made the transition to the jet on the slow scale, still, fast fluctuations will occur between the gyre and the jet, thus masking the signal as in Fig. 4. If the trajectory evolves towards the southern gyre, the fluctuations will happen only between southern gyre and jet.

This does not at all conflict with a probabilistic interpretation: The signal chooses randomly, according to the transition matrix and lifetime distribution a new state and lifetime. Information about history and details of the space evolution are forgotten (up to 1st order). This is the natural result of the coarse graining. The fast fluctuations are again random and follow their description with matrices and lifetimes. In our case, we find the trivial transition matrices, like in Eq. (12) due to the simplicity of the meandering jet system. In general, however, more complicated scenarios will appear.

In Fig. 8b we show the signal for  $\tau_f = 2$  and a model trajectory for the same parameters, as constructed by our method. In contrast to an older work [5] the signals resemble each other a lot, for comparison these results are reproduced in Fig. 8a.

Now we present some more quantitative comparisons. The first quantity to check is the information contained in the signals, it should be approximately the same, especially if we consider that this has been the main tool to find the models order. In Fig. 9 the comparison for  $\tau_f = 2$  and  $\tau_f = 12$  is shown – we find an excellent agreement.

Finally we check for the correlation function as the standard tool to investigate dependencies within the signal. The result is displayed in Fig. 10. The general behavior for the correlation functions is the same. It seems that the reconstructed ones slightly underestimate the correlations in the signal. There are two mechanisms leading to deviations of the construction from the original: firstly, the result depends sensitively on the correct estimation of the time scales involved in the original signal and secondly, the approximation of the pdf for the residence times by an exponential is nothing exact. Nevertheless, the coincidence is remarkably good, taking into account the possible error sources. For real-world applications, one should naturally calculate the pdf numerically and use the stored values.

## 6 Discussion and conclusion

In this paper we present a method to analyze and reconstruct multi-time-scale signals, which originate either from extended (after partitioning) or discrete systems. In our example, we use a simple partition of an extended system. To extract different time scales of the process, we apply the killing window filtering technique to the signal. With the filtered signals we use exit-time entropies to determine the Markovian order for the stochastic description of the process under consideration. With the information from the previous steps, we construct the multi time scale signal. The reconstructed signal shows good

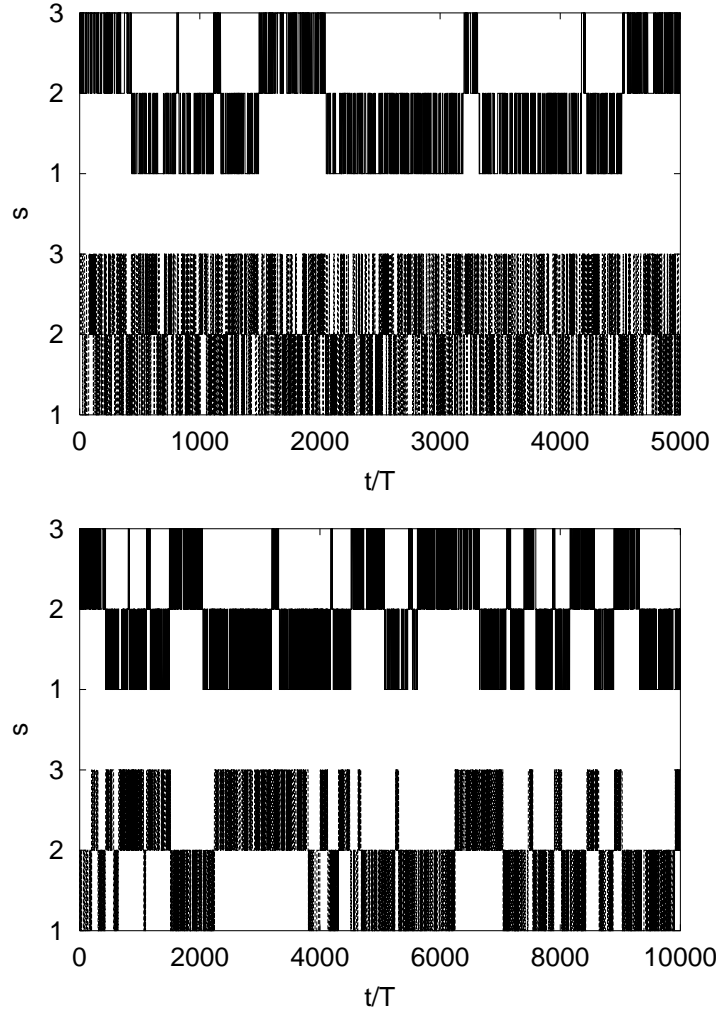


Figure 8: Comparison of the reconstructed signal with the true one. a) conventional construction, using fixed sampling time (cf. [5]). Upper part: original, lower part: construction. The slow scale transitions are not recovered and the signals differ a lot. b) signal as reconstructed by the Markovian cascade. Upper part: original, lower part: reconstruction. It is not obvious at once, which signal is the original one.

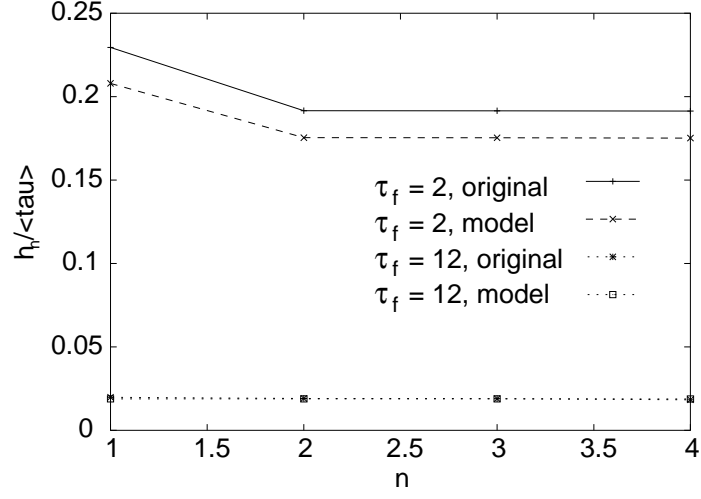


Figure 9: Comparison of the entropies calculated for the original signal and for the stochastic model.

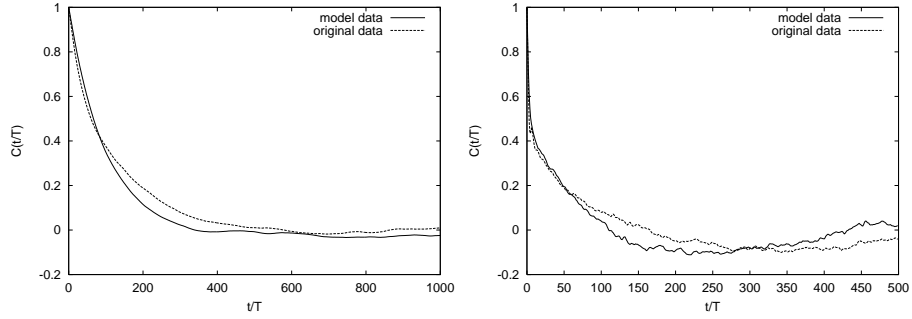


Figure 10: Left: correlation function for the filtered signal with  $\tau_F = 12$  and the corresponding reconstructed signal. Right: the same for  $\tau_F = 2$ . The rapid decay of the correlations is estimated very well by the model data.

statistical coincidence with the original data.

We did not investigate in detail the question about the amount of data needed for our method. This might vary from case to case, according to the conditions that are needed for the respective application. But error estimates are standard in this case and we do not expect novelties or surprises. The procedure is consistent as a whole, there are no ad-hoc assumptions necessary and everything is based purely on observations.

More general scenarios with more than two time scales involved are straightforward generalizations of the presented scheme, dependencies at a deeper level can be included easily, e.g., dependence of a fast time scale on the two preceding slower ones. This concept resembles the slaving idea [16, 17] which proved to be a powerful tool in pattern formation.

Applications are, to our opinion, mainly in the modeling and forecasting of signals. One can well imagine such a stochastic model as a minimal building block within a GCM or other simulation tools, which cannot resolve fine-scale temporal motion due to numerical restrictions. In this way, short-time fluctuations can be modeled by data analysis with signals from experimental data.

As a stand-alone tool, one can use the obtained information to predict the most probable track a tracer takes within a certain time, in this case the reconstruction method is only good for supervising the quality of the reconstruction.

It is hoped that these tools can be applied to real data. We think especially at data of the trajectories of Lagrangian tracers from oceanographic experiments. There, we have to occupy with finding the right partitioning of space. One can try to use ideas of dynamical systems theory, as e.g. described in [9]. These concepts however stand and fall with the amount and quality of data. If more information about the system is available to yield additional reasoning for specific partitions this should be used as input for a meaningful coarse-graining.

## 7 Acknowledgements

We thank A. Vulpiani for exchange of ideas and valuable discussions. Also M. Cencini, R. Pasmanter and D. Vergni have helped with interesting remarks. M.A. and K.H.A. have been partially supported by the EU network “intermittency in turbulence” (contract number FMRX-CT98-0175). G.L. has received support and hospitality from the University of Rome “La Sapienza”, Department of Physics. M.A. is currently supported by the DFG (German Research Foundation).

## References

- [1] M.C. Cross and P.C. Hohenberg. Pattern formation outside equilibrium. *Rev. Mod. Phys.*, 65:851–1112, 1993.

- [2] H. Kantz and T. Schreiber. *Nonlinear time series analysis*. Cambridge University Press, Cambridge, 1997.
- [3] C.W. Gardiner. *Handbook of Stochastic Methods*. Springer, New York, 1996.
- [4] H. v. Storch and F.W. Zwiers. *Statistical Analysis in Climate Research*. Cambridge University Press, Cambridge, UK, 1999.
- [5] M. Cencini, G. Lacorata, A. Vulpiani, and E. Zambianchi. Mixin in a meandering jet: a markovian approximation. *J. Phys. Oceanogr.*, 29:2578–2594, 1999.
- [6] J.D. Murray. *Mathematical Biology*. Springer, Berlin, 2nd edition, 1993.
- [7] A. Weisheimer, D. Handorf, and K. Dethloff. On the structure and variability of atmospheric circulation regimes in coupled climate models. *Atmospheric Sci. Lett.*, doi:10.1006/asle.2001.0034, 2001.
- [8] S. Corti and F. Molteni T. N. Palmer. Signature of recent climate change in frequencies of natural atmospheric circulation regimes. *Nature*, 398:799–802, 1999.
- [9] C. Coulliette and S. Wiggins. Intergyre transport in a wind-driven, quasi-geostrophic double gyre: An application of lobe dynamics. *Nonlinear Processes in Geophysics*, 8(1-2):69–94, 2001.
- [10] A. S. Bower. A simple kinematic mechanism for mixing fluid parcels across a meandering jet. *J. Phys. Oceanogr.*, 21:173–180, 1991.
- [11] R.M. Samelson. Fluid exchange across a meandering jet. *J. Phys. Oceanogr.*, 22:431–440, 1992.
- [12] B.V. Chirikov. A universal instability of many-dimensional oscillator systems. *Phys. Rep.*, 52:263–379, 1979.
- [13] M. Abel, L. Biferale, M. Cencini, M. Falcioni, D. Vergni, and A. Vulpiani. Exit-time approach to  $\epsilon$ -entropy. *Phys. Rev. Lett.*, 84(26):6002–6005, 2000.
- [14] M. Abel, L. Biferale, M. Cencini, M. Falcioni, D. Vergni, and A. Vulpian. Exit-times and  $\epsilon$ -entropy for dynamical systems, stochastic processes and turbulence. *Physica D*, 147:12–35, 2000.
- [15] If one turns the procedure round, to come from infinite filter length, we first find a range of constant information production while we are inside the slow scale only and end with a steep increase in information production when we arrive at the fast scale.
- [16] E. Ott. *Chaos in dynamical systems*. Cambridge University Press, Cambridge, UK, 1993.
- [17] H. Haken. *Synergetics*. Springer, New York, 3rd edition, 1983.



## 8 Appendix A

The calculation of the block entropy in Eq. 6 is valid for countable symbols. In this case, however the symbols are not countable, as each symbol involves a continuous variable; the residence time. The block entropy should therefore be calculated as

$$H^n = \sum \int d\tau p(S^n) \log(p(S^n)) , \quad (13)$$

where the sum extends over all possible permutations of n'th order. For practical purposes, the residence times have to be binned, the usual choice being a binning with resolution  $\tau_r$ . Then the block entropy turns, after renumbering all the possible words, into the sum  $H^n(\tau_r) = \sum p(S^n) \log p(S^n)$ , with summation over all possible words now in the now doubly discrete space. The entropy is found as

$$h(\tau_r)^n = \lim_{n \rightarrow \infty} H(\tau_r)^{n+1} - H(\tau_r)^n . \quad (14)$$

The limit of infinite time-resolution gives us the entropy *per exit*, i.e.:

$$h^n = \lim_{\tau_r \rightarrow 0} h^n(\tau_r) . \quad (15)$$

In Ref. [13, 14] more details are given, including the topics of continuous signals and several rigorous bounds for the entropy together with some applications.

